# μ-ARPES study of topological line-nodal compound CaSb₂

Chien-Wen CHUANG[1], Seigo SOUMA[2,3,*], Kosuke NAKAYAMA[1,4], Atsutoshi IKEDA[5], Mayo KAWAGUCHI[6], Keito OBATA[6], Shanta Ranjan SAHA[5], Hidemitsu TAKAHASHI[6], Shunsaku KITAGAWA[6], Kenji ISHIDA[6], Miho KITAMURA[7], Koji HORIBA[8], Hiroshi KUMIGASHIRA[9], Takashi TAKAHASHI[1] , Shingo YONEZAWA[6], Johnpierre PAGLIONE[5], Yoshiteru MAENO[6] and Takafumi SATO[1,2,3,10,**]

[1]Department of Physics, Graduate School of Science, Tohoku University, Sendai 980-8578, Japan
[2]Center for Science and Innovation in Spintronics, Tohoku University, Sendai 980-8577, Japan
[3]Advanced Institute for Materials Research (WPI-AIMR), Tohoku University, Sendai 980-8577, Japan
[4]Precursory Research for Embryonic Science and Technology (PRESTO),
Japan Science and Technology Agency (JST), Tokyo 102-0076, Japan
[5]Maryland Quantum Materials Center and Department of Physics, University of Maryland, College Park, Maryland 20742-4111, USA
[6]Department of Physics, Kyoto University, Kyoto 606-8502, Japan
[7]Institute of Materials Structure Science, High Energy Accelerator Research Organization (KEK), Tsukuba, Ibaraki 305-0801, Japan
[8]National Institutes for Quantum Science and Technology (QST), Sendai 980-8579, Japan
[9]Institute of Multidisciplinary Research for Advanced Materials (IMRAM), Tohoku University, Sendai 980-8577, Japan
[10]International Center for Synchrotron Radiation Innovation Smart, Tohoku University, Sendai 980-8577, Japan

## 1 Introduction

Recently, the superconductivity with superconducting transition temperature ($T_c$) of 1.7 K was discovered in a line-nodal compound CaSb₂ [1]. This material crystalizes in the monoclinic structure with P21/m space group with Sb zigzag chains running along the *b*-axis and mirror surfaces in the *a-c* plane, as shown in Fig. 1(a) [note that the bulk Brillouin zone (BZ) is shown in Fig. 1(b)]. First-principles band-structure calculations of CaSb₂ predicted the compensated semimetallic band structure [Fig. 1(c)] consisting of a 3D hole pocket extending roughly along the ΓX direction and quasi-two-dimensional (2D) cylindrical electron pockets axially centered along the YC line [top panel of Fig. 1(d)]. Band structure calculations predicted the presence of several Dirac points at specific k points such as Y, C, E, and A points (but not Γ and Z points which are related to the 3D pocket) due to the nonsymmorphic symmetry [2] [some of these Dirac points at the Y and C points are indicated by black arrows in Fig. 1(c)]. Such band crossings are connected to the line nodes at the $k_y = \pi$ plane [2] and one of them is associated with the shallow electron pocket crossing $E_F$, likely contributing to the transport properties, while these line nodes and Dirac nodes had to await experimental verification.

Magnetotransport measurements of CaSb₂ suggests the existence of line nodes [2], and specific heat measurements signified the deviation from the BCS behavior [3], suggestive of the unconventional nature of superconductivity. On the other hand, nuclear quadrupole resonance measurements suggested an exponential decrease in the inverse relaxation rate $1/T_1$ at low temperature, supportive of the conventional s-wave superconductivity with a full gap [4]. The presence of cylindrical electron pockets with line nodes has been discussed in favor of topological superconductivity [1] associated with the dominant interorbital pairing interaction with odd-parity pairing within the cylindrical FSs, similarly to the case of doped TIs [5] and doped Dirac semimetals [6,7]. To experimentally clarify the electronic states of CaSb₂ and to establish the interplay among nodal electrons, superconductivity, and topology, we have performed microfocused ARPES of CaSb₂ and clarifeed the 3D band structure and Fermi-surface (FS) topology [8].
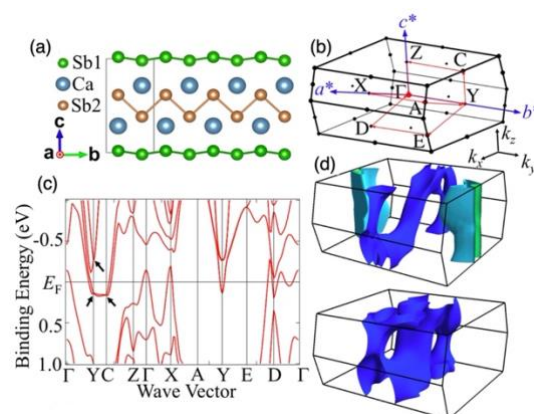


Fig. 1 (a) Crystal structure (side view) of CaSb₂. (b) Monoclinic bulk Brillouin zone (BZ) of CaSb₂. (c) Calculated band dispersions along high-symmetry lines in bulk BZ. (d) Calculated FSs in bulk BZ which incorporate (top panel) no μ shift and (bottom panel) downward μ shift of 210 meV.

## 2 Experiment

We prepared two different types of single crystalline samples for ARPES measurements, called here sample A and sample B. The samples A and B were grown by a self-flux method. For sample A, Ca (Sigma-Aldrich, 99.99%), and Sb (Alfa Aesar, 99.9999%) were melted at 1000 ∘C in an alumina crucible inside a sealed quartz tube, cooled down to 740 ∘ C, and then cooled down to 610 ∘C at a rate of −1∘C/h. Crystals were filtered in a centrifuge at this temperature. For sample B, Ca (Sigma-Aldrich, 99.99%) and Sb (Rare Metallic, 99.99%) were heated in a similar temperature profile but in a tungsten crucible. We found that typical size of the single-crystal domains is different between sample A (more than 1 mm size) and sample B (typically a few tens of μm). From the magnetic susceptibility measurements, we have confirmed the onset $T_c$ values of samples A and B to be ∼1.8 K [8].

We performed ARPES measurements at BL28A in KEK- PF [9]. We used circularly polarized photons of 30–300 eV. The energy and angular resolution was ∼20 meV and 0.2∘, respectively. The beam size on sample was $10 \times 12$ μm$^2$ [9]. Samples were kept at 40 K during measurements. The Fermi level ($E_F$) of samples was referred to that of a gold film deposited on the sample holder. A clear Laue pattern was observed for sample A, confirming the high single crystallinity of sample (note that it was difficult to obtain a clear Laue pattern for sample B due to the mixture of multiple crystal domains. However, we could safely determine the sample orientation for a small area of sample B on which the micro-ARPES measurement was performed, by looking at the periodicity and symmetry of obtained band structure). Since CaSb$_2$ single crystal was very hard to cleave, we tried cleaving several times in an ultrahigh vacuum (UHV), occasionally obtained a small flat area on the crystal with a few tens μm square and then focused the micro photon beam on it. The cleaving plane is *a-b* plane (perpendicular to the *c\** axis) according to our x-ray diffraction and ARPES data. We observed no signature of aging or contamination of sample surface during ARPES measurements.

## 3 Results and Discussion

Figure 2(a) shows the in-plane FS mapping at $T = 40$ K measured for sample B at hν = 90 eV which corresponds to the $k_z \sim 0$ plane. One can see a dominant intensity around the Γ point elongated along the $k_x$ direction. This feature originates from the Sb2-orbital-derived 3D hole pocket [2] as in the case of sample A, but its intensity distribution is different from that of sample A at $k_z \sim 0$ [8], likely due to the difference in their doping levels as detailed below. The existence of a hole pocket is recognized from the clear $E_F$ crossing of holelike band along a representative k cut (cut A) shown in Fig. 2(b). Besides the hole pocket, one can see in Fig. 2(a) a weak intensity around the Y point which is well separated from the hole pocket. Intriguingly, this feature is absent in sample A [8]. The ARPES intensity along k cut crossing this feature (cut B) in Fig. 2(c) signifies the existence of a shallow electron pocket around the Y point. The metallic electron pocket is also confirmed by the energy distribution

curve (EDC) at the Y point shown in Fig. 2(d) in which a peak near $E_F$ associated with the electron-band bottom accompanied with the Fermi edge cutoff is clearly seen. We have confirmed the existence of electron pocket also at hν = 120 eV, in line with its quasi-2D nature predicted from the calculation shown in Figs. 1(c) and 1(d). These results indicate that sample B is relatively more electron doped than sample A, and is situated in a semimetallic phase with both hole and electron pockets as predicted by the calculation for stoichiometric CaSb$_2$ (i.e., the calculation without μ shift). It is thus suggested that the absence of electron pocket in sample A [8] is not due to the experimental artifacts such as the strong intensity suppression associated with the matrix-element effect but due to the difference in the doping levels. This conclusion is also supported by the quantitative analysis of the experimental hole-band dispersion, the photoemission spectra in a wider energy range, and the Sb 4*d* core-level energies [8].
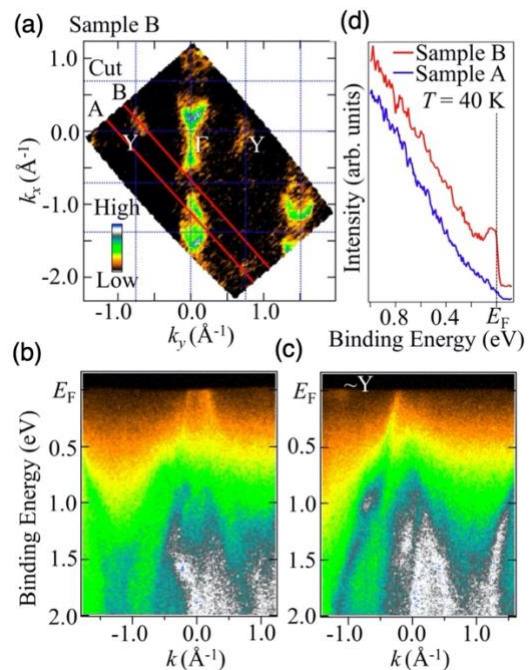


Fig. 2 (a) FS mapping at $T = 40$ K measured with hν = 90 eV (corresponding to $k_z \sim 0$ plane) for sample B. Blue lines indicate high-symmetry lines in surface BZ. Red lines indicate representative k cuts (cuts A and B) where the ARPES intensity shown in (b) and (c) was obtained. (b),(c) ARPES intensity as a function of wave vector and binding energy measured along cuts A and B, respectively. k in horizontal axis is defined as the distance between the measured k point and the intersection of red line and $k_x$ ($k_y$ = 0) axis. (d) EDC around the Y point which signifies the peak and metallic Fermi-edge cut-off associated with the electron pocket.

Our susceptibility measurements indicate that both samples A and B show superconductivity with almost the same onset $T_c$ of ∼1.8 K [8], despite the marked difference in the carrier-doping level. The fact that the FS of sample

A is composed only of the Sb2-derived 3D hole pocket at the $\Gamma$ point suggests that the main player of superconductivity is the hole carriers in this pocket. It is thus inferred that the electron carriers in the Sb1-derived quasi-2D FS centered at the Y(C ) point is not essential for the occurrence of superconductivity. This argument puts a constraint on the microscopic origin of superconductivity as well as its possible nontrivial nature in $CaSb_2$, because the occupancy of the electron band hosting the line nodes was suggested to be important for promoting topological superconductivity associated with the dominant interorbital pairing interaction with odd-parity pairing [1]. Also, it is worth noting that $CaSb_2$ maintains superconductivity regardless of the existence or absence of the electron pocket, which points to an intriguing possibility that one can tune the topological nature of superconductivity by simply controlling the carrier concentration in $CaSb_2$, although its validation needs further experimental studies that directly connects the fermiology and the superconducting pairing symmetry. We leave such an experiment as a challenge in future

References
[1] A. Ikeda, M. Kawaguchi, S. Koibuchi, T. Hashimoto, T. Kawakami, S. Yonezawa, M. Sato, and Y. Maeno, Phys. Rev. Mater. **4**, 041801(R) (2020).
[2] K. Funada, A. Yamakage, N. Yamashina, and H. Kageyama, J. Phys. Soc. Jpn. **88**, 044711 (2019).
[3] M. Oudah, J. Bannies, D. A. Bonn, and M. C. Aronson, Phys. Rev. B **105**, 184504 (2022).
[4] H. Takahashi, S. Kitagawa, K. Ishida, M. Kawaguchi, A. Ikeda, S. Yonezawa, and Y. Maeno, J. Phys. Soc. Jpn. **90**, 073702 (2021).
[5] S. Sasaki, M. Kriener, K. Segawa, K. Yada, Y. Tanaka, M. Sato, and Y. Ando, Phys. Rev. Lett. **107**, 217001 (2011).
[6] T. Kawakami, T. Okamura, S. Kobayashi, and M. Sato, Phys. Rev. X **8**, 041026 (2018).
[7] S. Kobayashi and M. Sato, Phys. Rev. Lett. **115**, 187001 (2015).
[8] C.-W. Chuang, S. Souma, A. Moriya, K. Nakayama, A. Ikeda, M. Kawaguchi, K. Obata, S. R. Saha, H. Takahashi, S. Kitagawa, K. Ishida, K. Tanaka, M. Kitamura, K. Horiba, H. Kumigashira, T. Takahashi, S. Yonezawa, J. Paglione, Y. Maeno, and T. Sato, Phys. Rev. Mater. **6**, 104203 (2022).
[9] M. Kitamura, S. Souma, A. Honma, D. Wakabayashi, H. Tanaka, A.Toyoshima, K. Amemiya, T. Kawakami, K. Sugawara, K. Nakayama, K. Yoshimatsu, H. Kumigashira, T. Sato, and K. Horiba, Rev. Sci. Instrum. **93**, 033906 (2022).

* s.souma@arpes.phys.tohoku.ac.jp
** t-sato@arpes.phys.tohoku.ac.jp

[1]